FAILURE ANALYSIS OF GAS TURBINE BLADES FOR UNDER WATER WEAPON

P.K. Sarma[1*], R. Srihari[2], V. Dharma Rao[3], K. Srinivas Rao[4], T. Subramaniam[4]
[1]GITAM University Visakhapatnam
[2]Scientist, NSTL, Visakhapatnam
[3]Gayatri Vidya Parishad Engineering College, Visakhapatnam
[4]Andhra University, Visakhapatnam
*Corresponding Author, Email: sarmapk@yahoo.com

ABSTRACT

The failure analysis of gas turbine blades at high rotational speeds is accomplished considering metallurgical, structural and thermal aspects. One of the reasons for the failure is found to be due to metallurgical phase transformations of the alloy at high temperatures. The blade material A718 Inconel transforms into δ- Phase and becomes susceptible to embrittlement at 650^0 C. Further the stresses developed at high rotational speeds of 50000 rpm exceed the yield strength and hence the rotational speeds must not exceed 40,000 rpm. The one dimensional transient thermal analysis is carried out by carefully adopting the thermal boundary conditions both at tip of the blade and root of the blade. For thermal ambience of the gas medium and rotational speeds, the blade temperature shoots up to very high values within a short time interval of 120 seconds. Hence it is suggested that the operating gas temperatures must be less than 500^0C and the rotational speeds must be in the range 30,000-40,000rpm for Inconel as the blade material to avoid failure.

Key words: gas turbine blades - A 718 inconel - δ phase – transient thermal study – structural failure

Introduction

Gas turbine technology is assuming paramount importance not only for stationary power generation but also for strategic purposes as a prime mover for under water weapons.

Gas turbine research assumed importance from early 1950. Several turbine blade cooling techniques have been developed transfer and related thermal problems because of shortage of high heat resistant alloys[1]. Several heat [2,3,4,5,6.7] have been investigated Metzger and Afghan [8] edited an excellent review on heat and mass transfer in rotating machinery.

In addition to compactness and associated high power to weight ratios, the prime mover should work reliably under varying system conditions. For example, in a specific case of under water weapon , the working fluid for the turbine is the products of combustion of a monopropellant fuel. This turbine experiences severe operating conditions in terms of pressure and temperature. In the ignition phase, turbine nozzle has an inlet temperature of more than 1000 ^{0}C and in the fuel burning phase the nozzle experiences inlet temperature of 1300 ^{0}C. This nozzle also experiences different operating pressures from low 60 bars to 200 bars, depending on the operating conditions...

This turbine rotor spins at very high speeds in the range of 50,000 RPM to 60,000 RPM. It is understood that at low speeds and at average temperatures the functioning of the rotor of the turbine is found to function well without any failure of the rotor system. However as the speed crosses a thresh hold or a critical value the turbine blades are totally getting sheared off from the root and the turbine fails Plate 1..is the proto type of the gas turbine rotor with turbine blades. After a few minutes of operation the gas turbine failed and some broken pieces of the turbine blades are shown in Photographic plate2

PLATE 1 - GAS TURBINE ROTOR WITH BLADES

PLATE No 2. BROKEN PIECES OF TURBINE BLADES

FIG.1. OPTICAL MICROGRAPH OF VIRGIN BLADE MATERIAL (200X)

The Purpose of the article is to look into the plausible reasons for the failure of the blades.It is believed that the failure is mainly due to the undue magnitude of thermal stresses induced at the root of the rotor when the rotor is subjected to operating speeds above critical values.

The following methodology is adopted in investigating the problem since it is likely that any of the following conditions through more light for the plausible reasons for the failure.

- Metallurgical investigations
- Stress analysis
- Thermal analysis

Metallurgical analysis

Super alloys have been employed for high temperature applications for aerospace industry in rocket engines, aircraft gas turbine parts etc. Among the super alloys, Inconel 718 is most extensively used as it possesses good strength, ductility and corrosion resistance up to 650^0C. It is a precipitation strengthened nickel based alloy developed by Eiselstein of the International Nickel company. 718 is extensively used in a wide range of aero engine applications such as turbine discs and turbine casing assemblies, high pressure compressor rotor drum assemblies, fuel nozzle rings, shafts, combustion liners. 718 also find major applications in nuclear, cryogenic and petrochemical industries. It is also finding a major application in the high temperature scramjet missile applications.

Experimental Details

In the present work two samples of gas turbine part made of IN718 alloy were supplied for investigations of the reasons for the failure. . One specimen is virgin material and the other is from failed part of the turbine. Samples were polished for microscopic examination and etched with the Kallings reagent (Composition 50mL HCL, 50mL Ethanol and 2.5gm $CuCl_2$). Micrographs were recorded with Olympus digital metallurgical microscope and are given in the Figs 1 and 2. Micrographs show clearly austenitic grains with twins.

FIG.2. OPTICAL MICROGRAPH OF FAILED BLADE MATERIAL (200X)

LITERATURE

The chemical composition (wt%) of 718 is as follows: Ni52, 18Fe, 18Cr, 3Mo, 5Nb, 1Ti, 0.5Al, 0.35Si, 0.35Mn, 0.04C, 0.004B. Chromium is added to improve corrosion resistance by forming Cr_20_3 layer and improve strength at elevated temperatures by forming chromium carbides [1, 2].Aluminum and titanium are added to precipitate high volume fraction of FCC γ' precipitates coherent with the austenitic γ matrix. Nb addition to greater than 4% results in the formation of a separate hardening phase γ''.Aluminum replaces chromium to some extent forming Al_2O_3 stable layer at elevated temperatures thus increasing the oxidation resistance in air and oxidizing atmospheres. Iron addition is unintentional for cost optimization and for improving malleability but increases susceptibility to deleterious sigma formation. Iron also reduces the oxidation resistance and restricts strengthening characteristics by limiting the solid solution and precipitation strengthening characteristics. Cobalt is added as a solid–solution strengthener and increases workability. The refractory elements namely niobium and molybdenum are added for solid – solution strengthening. They dissolve in the austenitic matrix and increase solvus temperature [3]. They reduce coarsening of γ' at service temperatures and participate in forming complex carbides. Boron is added to improve stress rupture properties. Silicon and manganese are added as de-oxidizers to promote workability and oxidation resistance. Carbon is added to form MC carbides that act as grain refiners during heat treatment operations.

Various Phases Present

718 contains basically austenitic matrix. The most common micro structural phases that are present in 718 are gamma prime (γ'), gamma double prime, (γ'') small amounts of TiC & TiN. Embrittling phases like Laves & Sigma are present as a result of poor ingot homogenization and long time exposure respectively (4).The various phases present in 718 are given in Table 1.

TABLE 1. SUMMARY OF VARIOUS PHASES IN INCONEL 718

Phase	Shape	Structure	Temperature Range of Precipitation °C	Minimum Niobium Content Required (Wt %)
MC	Cubic	-	1250 -1350	Above 80
Laves	Islands	HCP	650 - 1100	10-12
Delta	Needle like	Ortho rhombic	870-1010	6-8
γ''	Ellipsoidal/disc	BCT	700-890	4
γ'	Spherical	FCC	590-700	< 4

Austenite Matrix

The continuous matrix in an FCC nickel base austenitic phase (γ) contains high percentage of solid solution elements like chromium, cobalt, molybdenum & niobium etc. The reason attributed to the high strength, high temperature stability is due to the reasons such as high tolerance of nickel for alloying elements without phase instability, tendency to form chromium oxide layer Cr_2O_3 and also tendency to form Al_2O_3 which has exceptional resistance to oxidation.

Gamma Prime (γ')

It is an intermetallic phase responsible for precipitation strengthening formed in high nickel (> 25%) matrix super alloys. The γ' having a structure of A_3B type [Ni_3 (Al, Ti)] is a coherent phase with FCC structure. Strength of γ' increases with increasing temperature. The γ' contributes to strengthening by dislocation precipitate reaction. The morphology of γ' varies from spherical to cubical to elongated platelets depending upon the lattice mismatch. 718 contains approximately 4% γ' phase by volume fraction (5).

Gamma Double Prime (γ")

The predominant phase of strengthening in 718 is body centered tetragonal gamma double prime phase which precipitates coherently on {100} planes of the FCC matrix (1). The alloy contains about 15-20% of γ" by volume fraction (5). The γ" phase precipitates at relatively higher temperatures as ellipsoidal, disc shaped particles. The number of slip planes is less which contributes to the relatively high strength. The other reason for higher strength is due the distortion of the matrix caused by this phase.

Delta Phase (δ)

718 is susceptible to the formation of orthorhombic Ni_3N_b (δ) phase. Delta phase represents the thermodynamically stable form of metastable γ" phase. The δ phase requires minimum of about 6-8% Nb to form and precipitates over 870^0 C -1010^0 C temperature range with platelet morphology. It preferentially nucleates and grows at the grain boundaries along {111} planes in the matrix. It can also nucleate from the Nb enriched Laves phase during the solutionising treatment. The formation of large amount of more stable δ during long time exposure accompanied by γ" coarsening leads to degradation of properties due to loss of Nb from matrix. Also these reactions increase with the increase of the temperature resulting in the operating ceiling temperature of about 650^0C, and a limited service lifetime of the parts. It is there fore advisable to avoid exposure in excess of 650^0C.

Laves Phase

The Laves phase is a hard brittle intermetallic compound which forms in the γ matrix in the presence of elements like Nb, Ta, and Ti etc. The Laves phase is responsible for extended solidification temperature range and hot cracking susceptibility of the weld metal. From the above results and literature, exposure of 718 alloy to temperatures more than 650^0C may result in the formation of brittle Delta **Phase** (δ) at the austenitic grain boundaries. Delta phase causes crack nucleation and propagation which leads to catastrophic failure of the part made of 718 alloy. In the present case, failure of turbine blade may be attributed to the high temperature (more than 650^0C) exposure.

Calculation of Stresses on Rotating Disc

A rotating disc is subjected to stress induced by centripetal acceleration. A thin disc of radius R is considered, which rotates at an angular velocity . The radial stress (σ_r) and hoop stress (σ_θ). For the case of solid disc of uniform thickness without any external pressure acting on it the radial and hoop stresses are given by the following equations.

$$\sigma_r = \frac{3+\vartheta}{8}\rho\omega^2(R^2 - r^2) \qquad (1)$$

$$\sigma_\theta = \frac{\rho\omega^2}{8}[(3+\vartheta)R^2 - (1+3\vartheta)r^2] \qquad (2)$$

The maximum stress at the centre (at r = 0) is given by

$$\sigma_{r,max} = \sigma_{\theta,max} = \frac{3+\vartheta}{8}\rho\omega^2R^2 \qquad (3)$$

The properties for Inconel-718 are as follows.
Radius of the rotor disc, R = 0.119 m
Mass density, ρ = 8220 kg/m^3
Poisson's ratio, ν = 0.29
Rotational speed, N rpm
Angular velocity, ω = 2 π N / 60
From literature the following properties are available for INCONEL-718 at 600^oC.Ultimate tensile strength = 1067 MPa Yield strength (0.2% offset) = 890 MPa The maximum radial and hoop stresses are calculated from Eq. (3) for different rotational speeds, namely 60000, 70000 and 80000 rpm. The results are given below.

TABLE 2. RADIAL & HOOP STRESSES ON THE TURBINE BLADES AT DIFFERENT SPEEDS

S.No.	Speed of rotor disc (rpm)	Maximum Radial stress and Hoop stress ($\sigma_r = \sigma_\theta$) (MPa)
1	20000	210
2	40000	840
3	50000	1312
3	60000	1890

4	70000	2572
5	80000	3360

The following conclusions can be drawn from the results presented above.

1. The radial and hoop stresses developed at speeds above 50000 rpm exceed the yield strength and also the maximum tensile strength for inconel-718.
2. The allowable maximum stresses at the disc-to-blade joint could be less than those on the disc.
3. Hence failure can occur due development of high stresses on the disc and at the disc-to-blade joint.

Thermal Analysis

The metallurgical studies further lead to the thermal analysis to which the gas turbine blade is subjected to transient thermal conditions. The heat transfer to the rotating surfaces from the hot ambient medium can be estimated from the studies conducted by the authors [6, 7 & 8]. The estimated values of the heat transfer coefficient for the ranges of operating conditions of the turbine would be 100 – 400 W/m^2 K.

Applying principles of conservation of energy to the control volume shown in figure3 the it follows

$$[h_i - h_o] - [Q_1 + Q_2] = W \qquad (4)$$

[CHANGE IN ENTHALPY] – [HEAT LOSSES]= [MECHANICAL POWER OUTPUT]

The change in enthalpy is

$$[h_i - h_o] = \dot{m}[C_P(T_i - T_o)] \qquad (5)$$

Thermal losses $[Q_1 + Q_2]$ are the heat conduction losses at the extremities of the gas turbine blade i.e., at the tip and base of the blade and the rotor of the turbine The mechanical power output from the turbine is

$$W = \eta[h_i - h_o] \qquad (6)$$

where η is mechanical efficiency.

Thus, $[Q_1 + Q_2] = [1 - \eta](h_i - h_o)$ (7)

If the tip lossesQ_1=0 are negligible the heat losses at the base of the blade

Q_2= [1-η] (h_i-h_o) (8)

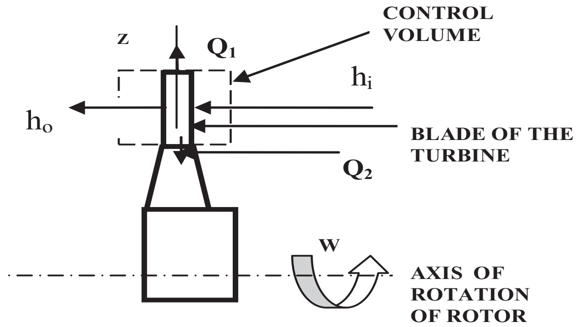

FIG3.CONTROL VOLUME CONFIGURATION

Equation(5) can be considered as as one of the boundary conditions in the evaluation of transient thermal conditions of the blade i.e., for the coordinate system shown in figure(1)

$$Q_{Z=0} = -kA \left.\frac{\partial T}{\partial Z}\right|_{Z=0} \qquad (9)$$

UNSTEADY STATE HEAT TRANSFER IN TURBINE BLADE AND ROTOR DISC

Physical Model

A gas turbine is considered which contains a circular rotor disk of radius R. The blades each of length L are mounted on the rotor disc at its radius, i.e., at r = R. The turbine blades and rotor disc are initially at a temperature of T_i. At time zero, a hot gas at a temperature T_g is injected onto the turbine blades thus causing rotation of the rotor disc at a high speed of 60000 rpm. Heat is transferred from the hot gas to the tip of each blade (at x = 0) by forced convection. Heat is transferred from the blade tip (x = 0) to root (x = L) by conduction. The root of the blade is connected to the disc at its radius, heat is conducted into the disc towards its central axis (r = 0) by conduction. The convective heat transfer coefficient for the case of a rotating disc is of the order of 150 W/m^2-K. Thus the problem of unsteady state heat transfer in the turbine is subdivided into two problems, viz., conduction heat transfer in the blade, and that in the rotor disc. The heat received at the root of the blade becomes the input to the rotor disc.

Mathematical Formulation of the Problem

Unsteady state heat transfer in the turbine blade

The heat transfer through the blade is governed by the equation of unsteady state two-dimensional heat conduction as given below.

$$\rho C \frac{\partial T}{\partial t} = k \frac{\partial^2 T}{\partial x^2} - h \frac{P}{A}\left(T_g - T\right) \qquad (10)$$

where P and A are the perimeter and cross sectional area of the blade respectively.

Initial and Boundary Conditions

Initially, i.e., at t = 0, the temperature of the blade is equal to Ti through out.

$T = T_i$ for $0 \le x \le L$ at t = 0. For t>0:

The gas is at a constant temperature T_g. Heat is transferred by convection from the gas to the tip of the blade.

$$-k \frac{\partial T}{\partial x} = h\left(T_g - T_0\right) \text{ at } x = 0 \text{ (tip)} \qquad (11)$$

where T_0 is the temperature at the tip of the blade, i.e., at x = 0.

$$-k \frac{\partial T}{\partial x} = q_{root} \quad \text{at } x = L$$

where is q_{root} the heat flux at the root of the blade, i.e., at x = L.

Unsteady state heat transfer in the circular rotor disc

The heat transfer through the rotor disc is governed by the equation of unsteady state two-dimensional heat conduction as given below.

$$\rho C \frac{\partial T}{\partial t} = k \frac{\partial}{\partial r}\left(\frac{\partial T}{\partial r}\right) \qquad (12)$$

Initial and Boundary Conditions

Initially, i.e., at t = 0, the temperature of the disc is equal to T_i through out.

$T = T_i$ for $0 \le r \le R$ at t = 0.

For t>0:

The temperature at the root of the blade is equal to the temperature at the radius of the disc.

$$T\big|_{x=L} = T\big|_{r=R}$$

Heat is transferred by conduction from the blade to the disc at the root of the blade.

$$-k \frac{\partial T}{\partial r} = q_{root} \quad \text{at } r = R$$

The temperature derivative at the centre of the disc is equal to zero by symmetry.

$$-k \frac{\partial T}{\partial r} = 0 \quad \text{at } r = 0$$

Numerical Solution Method

Both the problems of unsteady state heat transfer in the blade as well as in the rotor disc contain convection heat transfer from gas to the solid and subsequent heat transfer within the solid by conduction. Both of them are formulated presently as one dimensional unsteady state problem. While the problem of blade is in Cartesian coordinates that of the rotor disc is in cylindrical coordinates.

Both the problems are solved numerically by using Crank-Nicolson implicit scheme. In this method the total length of blade is divided into a number of grids, such that the grid length Δx is given by the length of the blade divided by the number of grids. A time increment Δt is considered. The unsteady state heat conduction equation is written in discretized (finite difference) form using the temperatures at the nodes. Both the temperatures at the current time, t and the new temperatures at time $(t+\Delta t)$ appear in the discretized equation. This equation is rearranged to obtain a tridiagonal matrix containing thee new temperatures at adjacent nodes in each equation. The temperatures at the tip (x = 0) and root (x = L) of the blade are determined (or, expressed in terms of the adjacent temperature at the intermediate node) by using the boundary conditions, which are provided above. The tridiagonal matrix contains the temperatures at all the intermediate nodes (i.e., except at the tip and root of the blade). The TDMA is solved by using Thomas algorithm to get the temperatures at all the intermediate nodes. The temperatures at the ends are evaluated making use of the obtained temperatures. Thus the temperatures at time $(t+\Delta t)$ are obtained. An increment in time is considered and the same procedure is adopted to find temperatures at time $(t+2\Delta t)$. The procedure is continued until no appreciable change is observed in the temperatures at all nodes at two successive increments in time. Then it is established that the steady state is obtained. The solution is stopped.

The rotor disc along its radius is also divided into a number of grids so that the grid size is equal to Δr. The temperatures on the rotor disc are also obtained using Crank-Nicolson implicit scheme. The same procedure as illustrated above is applied to obtain temperatures at all grid points on the rotor disc also at different time increments until steady state is attained. The detailed procedure is available in the program source code.

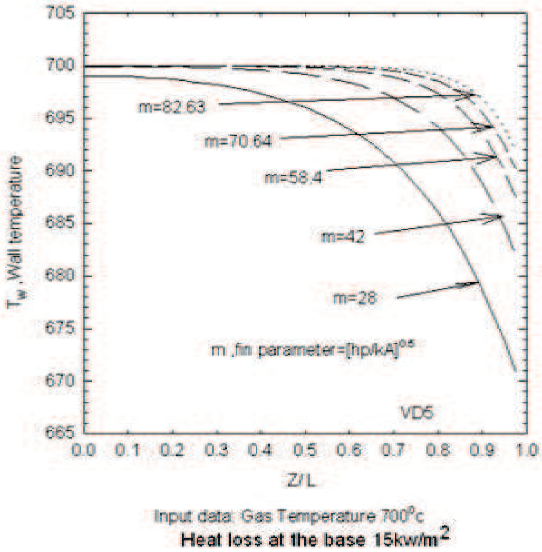

FIG4. STEADY STATE TEMPERATURE ALONG THE BLADE FOR DIFFERENT FIN PARAMETERS

Figure (4) depicts the steady state one dimensional temperature in the blade for the input data shown in the figure. The transient thermal variations for different input conditions are further displayed in figures (5, 6, and 7). Evidently with in a short span of time less than a minute the blade temperatures get elevated to high temperatures leading to metallurgical transformations that promote failure.

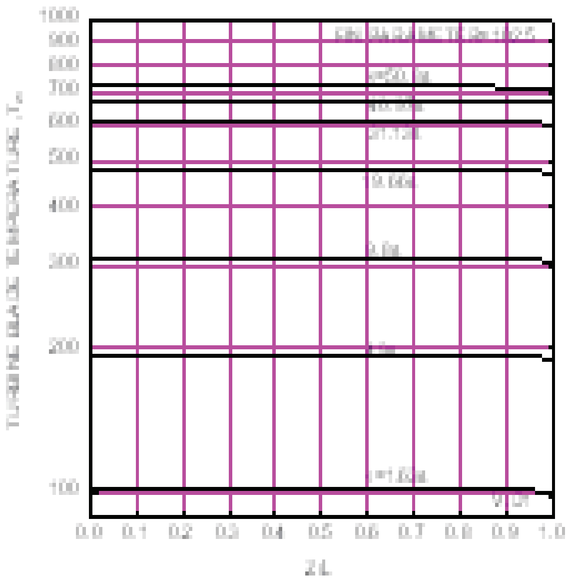

FIG5. VARIATION OF BLADE TEMPERATURE ALONG THE TIP

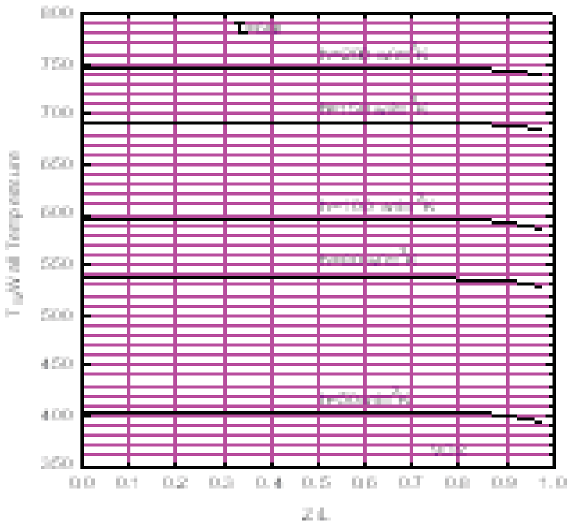

FIG6. EFFECT OF HEAT TRANSFER COEFFICIENT ON WALL TEMPERATURE

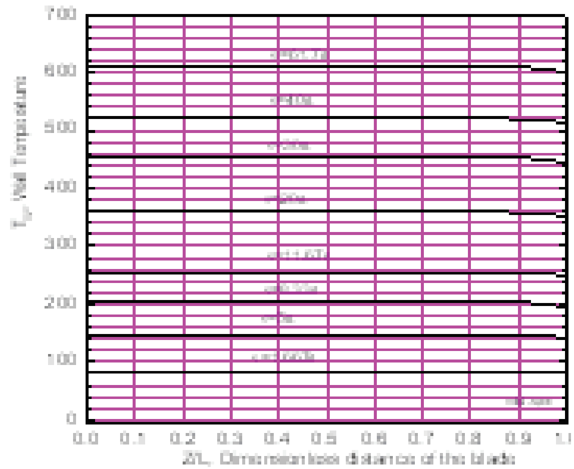

FIG7. VARIATION OF BLADE TEMPERATURE ALONG ITS LENGTH WITH TIME

Conclusions

1. Avoid metallurgical transformations leading to failure due to transformation into delta phase.
2. The stress analysis computations at speeds 30,000 rpm to 50,000 rpm are well within the yield strength of A-718m inconal and The turbine must operate at low pressures and at moderate temperatures 500^0C - 600^0 C to hence the rotational speeds are not be considered as valid reasons for failure as long as the rotational speeds do not exceed 50,000rpm.
3. The thermal analysis with the help of Fourier conduction equation revealed that the blade shoots up to high temp of ambient gas medium within less than 60S for ambient temperatures in the ranges 600^0 C – 700^0C. This particular range is very detrimental for the A-718 in and to transform to Delta 8 –phase.

The results from the computer program for the following ranges of operating conditions are provided in the article.

Gas temperature 600^0C - 800^0C

Initial temperature range of turbine blade = 30^0C - 50^0C

Overall that transfer coefficient – 150 -350 W/m^2 k.

Heat loses at the base of the blade to the core = 10 – 30(KW/m^2)

Nomenclature

A	cross sectional area of tube, (m^2)
C_p	specific heat, (J/kgK)
D	diameter of the tube, (m)
f	friction coefficient
h	Enthalpy, kJ/kg
h	heat transfer coefficient,(W/ m^2 K)
K	thermal conductivity, (W/mK)
L	mixing length, (m)
$\overset{*}{m}$	mass flow rate, (kg/sec)
N	Speed of the Rotor, RPM
Nu	Nusselt number, $\left(\frac{hD}{k}\right)$
P	Pressure, Bar
p	perimeter, m
Pr	Prandtl number, $\left(\frac{\mu C_p}{k}\right)$
Q	heat, (W)
r	radial direction
R	radius of the rotor, (m)
t	Time, s
Δt	time increment, s
T	temperature, (C)
W	Work, (W)
τ	Shear stress, N/m^2
ω	Angular Velocity, Rad/s
σ_θ	hoop stress, N/m^2

Greek symbols

ν	Poisson's Ratio
ρ	Density, (kg/m^3)
η	Efficiency
σ_r	radial stress, N/m^2

Subscripts

i	inlet
f	fluid
g	gas
m	mean
o	outlet

REFERENCES

1. Chaturvedi M.C. and Han Y, (1983) Strengthening Mechanisms in Inconel 718 Superalloy, *Mater. Sci*., 17, p145-149.
2. Douglas D.L., (1971) "Fundamentals of the Reactions Between Metals and Their Environment At High Temperatures",SAMPE 16th *National symposium*.
3. Kriege O.H. & J.M. Baris, (1969) *Trans ASM*, Vol 62, March, p.195-200.
4. Krugger D.D., (1989) The Development Of Direct Age 718 For Gas Turbine Disk Applications, *Conf. Proc. On 718*, TMS, Edited by E.A. Loria.
5. Paulonis D.F., J.M.Oblak and D.S. Duvall, (1969) *Trans. Of ASM,* 62, p.611.
6. Mahmood Farzaneh-Gord, Heat Transfer over Rotor Surface in a Pre-swirl Rotating-Disc System, International Journal of Dynamics of Fluids, Vol. 3, Number 1 (2007), pp. 81–94
7. G. Cardone, T. Astarita and G.M. Carlomagno, Infrared heat transfer measurements on a rotating disk, Optical Diagnostics in Engineering Vol. 1(2)(1996), 1-7
8. V. G. Rifert, Analysis of the Heat Transfer during Evaporation from a Rotating Disk, Polytechnic Institute, Kiev. Translated from *Inzhenerno-Fizicheskii Zhurnal*, Vol. 25, No. 2, pp.232-236, August, 1973. Original article submitted June 20, 1972.

APPENDIX:

Physical Properties: A718

Density: 8.19 g/cm3

Melting point/Range: 1260 – 1336 ^{0}C

Specific Heat: 435 J/kg K

Average Coefficient of Thermal Expansiom: 13.0

µm/m · K

Thermal Conductivity: 1.4W/m K

Electrical Resistivity: 1250 n · m